ChemPhysChem

Chemistry Europe
European Chemical Societies Publishing

Accepted Article

Title: Singlet-triplet excited-state inversion in heptazine and related molecules: assessment of TD-DFT and ab initio methods

Authors: Gaetano Ricci, Emilio San-Fabián Maroto, Yoann Olivier, and Juan-Carlos Sancho-Garcia

To be cited as: *ChemPhysChem* 10.1002/cphc.202000926

Link to VoR: https://doi.org/10.1002/cphc.202000926

WILEY-VCH

10.1002/cphc.202000926

Singlet-Triplet Excited-State Inversion in Heptazine and Related Molecules: Assessment of TD-DFT and *ab initio* Methods

G. Ricci[a], Prof. E. San-Fabián[b],
Prof. Y. Olivier[a], and Prof. J. C. Sancho-García[b*]

[a] Unité de Chimie Physique Théorique et Structurale
& Laboratoire de Physique du Solid,
Namur Institute of Structured Matter,
Université de Namur,
B-5000 Namur, Belgium

[b] Department of Physical Chemistry,
University of Alicante,
E-03080 Alicante, Spain

December 14, 2020

*E-mail: jc.sancho@ua.es

Abstract

We have investigated the origin of the S_1-T_1 energy levels inversion for heptazine, and other N-doped π-conjugated hydrocarbons, leading thus to an unusually negative singlet-triplet energy gap ($\Delta E_{ST} < 0$). Since this inversion might rely on substantial doubly-excited configurations to the S_1 and/or T_1 wavefunctions, we have systematically applied multi-configurational SA-CASSCF and SC-NEVPT2 methods, SCS-corrected CC2 and ADC(2) approaches, and linear-response TD-DFT, to analyze if the latter method could also face this challenging issue. We have also extended the study to B-doped π-conjugated systems, to see the effect of chemical composition on the results. For all the systems studied, an intricate interplay between the singlet-triplet exchange interaction, the influence of doubly-excited configurations, and the impact of dynamic correlation effects, serves to explain the $\Delta E_{ST} < 0$ values found for most of the compounds, which is not predicted by TD-DFT.

Key words: Singlet-triplet energy gap; heptazine derivatives; electron correlation effects; TD-DFT; SA-CASSCF; SC-NEVPT2; SCS-CC2; SCS-ADC(2).

1 Introduction

Heptazine (also commonly known as tri-*s*-triazine and composed of three fused triazine rings) consists on a triangular core with N-substituted sites and it was first synthesized in 1982 [1]. There is now a renewed interest in heptazine derivatives as precursors of N-rich carbon nitrides [2, 3], building blocks of photocatalytic porous polymer networks [4, 5], and efficient light-emitters [6, 7] in Organic Light-Emitting Diodes (OLEDs), among other envisioned applications. Besides, and more generally speaking, N- and B-doped triangulene-based compounds, such as DABNA-1 or TABNA [8–10], present unique features with high interest for optoeletronics applications, such as narrow emission and high quantum yield, while displaying Thermally Activated Delayed Fluorescence (TADF). These properties are driven by short-range charge-transfer [11], which spatially separate the hole and the electron densities on neighbouring atomic sites while ensuring a high polarizability [12]. Oligomerization of heptazine is also a promising and versatile route towards catalysis for hydrogen production and water splitting [13–15] and CO_2 uptake [16], as well as substitution at the corners to improve the photocatalytic performance [17]. This scenario allows to foresee a blooming of studies for energy conversion and storage, as well as for industrial and environmental applications of heptazine derivatives and oligomers [18, 19].

Particularly interesting from both an experimental and theoretical point of view, e.g. in the search of more efficient photophysical applications, is the location of the lowest singlet and triplet excited-state energy levels of triangular shape molecules. Recent interesting works have shown a violation of Hund's multiplicity rule in N-doped triangulenes, namely cyclazine and heptazine, with the lowest triplet excited-state (T_1) found higher in energy

than the lowest singlet excited-state (S_1) contrarily to almost all known closed-shell organic molecules [20, 21]. Violation of Hund's rule has been studied before, mostly for establishing the correct spin multiplicity of the ground-state [22, 23], and it can occur for π-conjugated hydrocarbons with a bipartite lattice. The triangle-shaped topology of heptazine and related molecules could certainly play some role [24] but the importance of on-site heterosubstitution with N atoms, and how closely related molecules could obey or not the Hund's rule, deserves to be further investigated to establish structure-property relationships [25]. We have thus selected a set of N-substituted hydrocarbons with a triangle-like shape, see Figure 1, and carefully applied state-of-the-art excited-state methods to obtain the desired energy levels. We will also extend the study to other closely related molecules, including some B-doped examples, to further discuss the effect of chemical susbtitution.

Concerning the methods choice, Time-Dependent Density-Functional Theory (TD-DFT) [26–29] has been shown unable before to provide for these molecules the correct order of the states, independently of the exchange-correlation functional selected [20, 21]. Generally speaking, the global accuracy of TD-DFT is out of question, as well as its excellent trade-off between accuracy and computational cost for real-world applications, but these are also examples for which the adiabatic approximation (i.e., frequency-independent kernels) introduces some limits [30]. This issue is further explored here, hopefully complementing previous studies [20, 21] after inspecting first the corresponding theoretical expression in which the TD-DFT singlet-triplet gap is based. Additionally, we will try to provide insights, beyond the one-electron molecular picture [31], to understand why (highly)

correlated methods are able to cope with the underlying electronic structure of these systems, and thus predicting the correct order and energy of excited-states, contrarily to what happens with TD-DFT. This theoretical understanding could pave the way towards the theoretical design of other closed-shell organic molecules with inverted excited-states and therefore with prospects in optoelectronic and photocatalytic applications.

2 Theoretical framework

2.1 Explicit expression from the TD-DFT method

One central aspect of the present work is to demonstrate if the inversion of S_1 and T_1 states can be predicted or not accurately by TD-DFT: we thus present first the expression used for the corresponding energy difference, ΔE_{ST}, to understand the origin of its performance. Upon a linear-response regime, the excitation energies (Ω) between ground- and excited-states arise from the solution of the non-Hermitian eigenvalue problem [32]:

$$\begin{bmatrix} \mathbf{A} & \mathbf{B} \\ \mathbf{B}^\star & \mathbf{A}^\star \end{bmatrix} \begin{bmatrix} \mathbf{X} \\ \mathbf{Y} \end{bmatrix} = \Omega_{\mathrm{TD-DFT}} \begin{bmatrix} \mathbf{1} & \mathbf{0} \\ \mathbf{0} & -\mathbf{1} \end{bmatrix} \begin{bmatrix} \mathbf{X} \\ \mathbf{Y} \end{bmatrix}, \tag{1}$$

with $\mathbf{X}$ ($\mathbf{Y}$) the set of (de-)excitation amplitudes. Occupied (unoccupied) orbitals are denoted in the following as i, j (a, b). We can introduce in the expression(if needed) the weight (C_x) of the HF-like exchange term entering into the hybrid form of the exchange-correlation hybrid functional, $E_{xc}[\rho]$, chosen. A pure (semi-local) functional will have consequently $C_x = 0$. The spinless matrix elements of the orbital rotation Hessians matrices $\mathbf{A}$ and $\mathbf{B}$ are given by:

$$A_{ia,jb} = \delta_{ij}\delta_{ab}(\epsilon_a - \epsilon_i) + (ia|jb) - C_x(ij|ab) + (1 - C_x)\,(ia|\hat{f}_{xc}|jb) \tag{2}$$

$$B_{ia,jb} = (ia|bj) - C_x(ib|aj) + (1 - C_x)\,(ia|\hat{f}_{xc}|bj), \tag{3}$$

with ϵ the energy eigenvalue, $(ia|jb)$ the integral $\iint \phi_i^\star(\mathbf{r})\phi_a(\mathbf{r})\frac{1}{|\mathbf{r}-\mathbf{r}'|}\phi_j^\star(\mathbf{r}')\phi_b(\mathbf{r}')d\mathbf{r}d\mathbf{r}'$, which could take an exchange-type, $(ia|jb)$ or simply K, or as a Coulomb-type form, $(ij|ab)$; and $(ia|\hat{f}_{xc}|jb)$ the integral $\iint \phi_i^\star(\mathbf{r})\phi_a(\mathbf{r})\hat{f}_{xc}(\mathbf{r},\mathbf{r}',\omega)\phi_j^\star(\mathbf{r}')\phi_b(\mathbf{r}')d\mathbf{r}d\mathbf{r}'$, with $\hat{f}_{xc} = \frac{\delta^2 E_{xc}[\rho]}{\delta\rho(\mathbf{r})\rho(\mathbf{r}')}$ the (approximate) exchange-correlation kernel. Note that: (i) in the adiabatic approximation mostly used in practice, $\hat{f}_{xc}$ is made frequency-independent and it thus reduces to $\hat{f}_{xc}(\mathbf{r},\mathbf{r}')$; and (ii) the term $(ia|\hat{f}_{xc}|bj)$ is often negative [33] with a magnitude depending on each system and the exchange-correlation functional chosen.

The Tamm-Dancoff approximation [34] sets $\mathbf{B} = 0$ in the full TD-DFT equations; Eq. (1) thus becomes $\mathbf{AX} = \Omega_{\mathrm{TDA-DFT}}\mathbf{X}$, with the matrix elements simplified (setting also $C_x = 0$) to:

$$A_{ia,jb} = \delta_{ij}\delta_{ab}(\epsilon_a - \epsilon_i) + (ia|jb) + (ia|\hat{f}_{xc}|jb). \quad (4)$$

Note that: (i) in contrast to the Configuration Interaction Singles (CIS) formalism, any TD(A)-DFT result will also depend on the $(ia|\hat{f}_{xc}|jb)$ term; and (ii) the CIS method is recovered by replacing the last term by $-(ij|ab)$. Since our main interests is the singlet-triplet energy difference, and taking into account that most excitations in conjugated systems are dominated by the $(i \rightarrow a)$ orbital transition, it thus becomes in its simplest form:

$$\Delta E_{ST} \approx 2(ia|jb) + 2(ia|\hat{f}_{xc}|jb). \quad (5)$$

Note that this result was previously emphasized on Refs. 11 and 20, for a necessarily simplified "two-state model". For TDA-DFT, the second term in Eq. (5) is expected to decrease the ΔE_{ST} values. Thus, potentially, ΔE_{ST} could be negative depending on the relative magnitude of $|(ia|\hat{f}_{xc}|jb)|$ vs. $(ia|jb)$, since two-electron integrals (first term) are positive definite.

2.2 Computational details

All the structures were optimized by the B97-3c method [35], unless some exception for which the HF-3c method [36] was used instead, obtaining rigid and completely planar geometries with all-real $(3N-6)$ vibrational frequencies. Then, we calculated (vertical) relative energies between ground- and lowest excited-state of singlet (S_1) and triplet (T_1) multiplicity, $S_1 \leftarrow S_0$ and $T_1 \leftarrow S_0$ respectively, giving rise to the singlet-triplet energy difference always calculated as $\Delta E_{ST} = E(S_1 \leftarrow S_0) - E(T_1 \leftarrow S_0)$. Relaxing the geometrical structures of the S_1 and T_1 states is not expected to have any influence due to the rigidity of the molecular backbone [12]. We carried out Time-Dependent DFT calculations (TD-DFT) together with the Tamm-Dancoff approximation (TDA-DFT) [34], with PBE-based exchange-correlation functionals [37, 38]. However, the conclusion are not expected to differ upon employing any other approximation (e.g. the M06-2X [39] and ωB97XD functionals [40] are also explored). The multi-configurational Complete Active Space Self-Consistent Field (State-Averaged) (SA-)CASSCF and N-electron Valence second-order Perturbation Theory (Strongly-Contracted) (SC-)NEVPT2 [41–43] methods employed an increasingly larger (N, M) active space of N electrons in M orbitals, to discard any qualitative influence of the active space selection, and always demanded the same number of roots of each multiplicity (S_n and T_n). Note that for simplicity we do not include possible $N \neq M$ active spaces. These calculations are done in conjuction with natural orbitals obtained at a first step at the second-order Møller-Plesset perturbation theory (MP2). To be sure that the results remains independent of the technicalities of the methods selected, we also performed another set of *ab initio* calculations: (i) Configuration Interaction Singles, CIS, also approximately corrected with Double

excitations, CIS(D); (ii) Second-order approximate Coupled Cluster singles and doubles model, CC2 [44,45]; and (iii) Second-order Algebraic Diagrammatic Construction, ADC(2) [46]. Note that for CC2 and ADC(2) the Spin-Component-Scaling (SCS-) correction was employed [47] to account for missing correlation effects upon scaling the same and opposite spin-components separately. The TDA-DFT, CIS, SA-CASSCF, and SC-NEVPT2 calculations are done with the ORCA 4.0 package [48]; CIS(D), SCS-CC2, and SCS-ADC(2) are instead done with the TURBOMOLE 7.4 package [49]. We fixed the def2-TZVP basis set [50] for all the calculations, which were done with the Resolution-of-the-Identity (RI) approximation [51], together with the corresponding auxiliary basis sets [52] def2/JK and def2-TZVP/C.

2.3 Previous evidences of $\Delta E_{ST} < 0$ for heptazine and its derivatives

Next, we will summarize the available experimental and theoretical information about these systems. Recent experimental studies on heptazine (actually a substituted heptazine but with substituents attached to the corners weakly affecting its electronic structure and photophysics) clearly evidenced the inversion of S_1 and T_1 states [21] from the observed long lifetime of the S_1 state in presence or in absence of molecular oxygen which is expected to quench triplet excited states. Prompt and delayed fluorescence has been also demonstrated on several heptazine derivatives [53]. Note also that the absorption spectra of other N-doped 2T-N and 2T-4N compounds were also measured in the past [54,55], with the energy location of the triplet state being still challenging. Actually, it was also experimentally found a very short lifetime of the T_1 state of 2T-4N [55], compatible with a radiationless intersystem crossing $S_1 \leftarrow T_1$ and thus isoenergetic energy levels.

From a theoretical point of view, previous estimates of ΔE_{ST} at different sophisticated theoretical levels such as RAS-SF, ADC(2), and EOM-CCSD predicted values between –0.10 and –0.16 eV for 2T-N [20,56], while ADC(2), CC2, EOM-CCSD, and CASPT2 methods predicted ΔE_{ST} energies between –0.18 and –0.28 eV for 2T-7N [21].

3 Results and discussion

3.1 Understanding the performance of the TD-DFT method

To quantitatively corroborate the arguments exposed above about the (possible) inability of CIS and TDA-DFT methods to predict a $\Delta E_{ST} < 0$ value for these systems, a preliminary calculation of ΔE_{ST} by CIS for the three compounds selected, see Table 1, leads to:

$$\Delta E_{ST}^{\mathrm{CIS}}(\text{2T-N}) = 0.337 \text{ eV} \quad (6)$$

$$\Delta E_{ST}^{\mathrm{CIS}}(\text{2T-4N}) = 0.685 \text{ eV} \quad (7)$$

$$\Delta E_{ST}^{\mathrm{CIS}}(\text{2T-7N}) = 0.410 \text{ eV}. \quad (8)$$

If the simplest "two-state" model, see Ref. 25 for details, was used that would lead to a value of K, often referred as the "exchange energy" comprised between $0.17 - 0.34$ eV, and thus slightly smaller than the values of around $0.4 - 0.5$ eV commonly found in π-conjugated polymers [57]. However, that is a rough approximation for K only valid for a model with singlet and triplet states sharing the same electron configuration but different spin. For a more robust expression, as that arising from a more extended "four-state" model see also Ref. 25. These small values (in a simplified view) are believed to arise from a minor overlap between the frontier occupied and virtual orbitals and helped to explain, for instance, former strategies to decrease the ΔE_{ST} values by relying on the Donor-Acceptor (D-A) fragment

strategy [58], of interest for the field or organic light-emission [59]. Actually, Figure 2 presents the disjoint nature of both the Highest Occupied and Lowest Unoccupied Molecular Orbitals (HOMO and LUMO) for this set of compounds, easily seen the different spatial location of the lobes and their expected poor overlap.

If one performs a TDA-DFT calculation with just the PBE exchange functional, thus neglecting ($\hat{f}_c = 0$) the corresponding correlation functional, we obtain:

$$\Delta E_{ST}^{\mathrm{TDA-PBEx}}(\text{2T-N}) = 0.195 \text{ eV} \quad (9)$$

$$\Delta E_{ST}^{\mathrm{TDA-PBEx}}(\text{2T-4N}) = 0.274 \text{ eV} \quad (10)$$

$$\Delta E_{ST}^{\mathrm{TDA-PBEx}}(\text{2T-7N}) = 0.202 \text{ eV}, \quad (11)$$

while if we perform now the the corresponding TDA-DFT calculation, including now both PBE exchange and correlation terms:

$$\Delta E_{ST}^{\mathrm{TDA-PBE}}(\text{2T-N}) = 0.187 \text{ eV} \quad (12)$$

$$\Delta E_{ST}^{\mathrm{TDA-PBE}}(\text{2T-4N}) = 0.260 \text{ eV} \quad (13)$$

$$\Delta E_{ST}^{\mathrm{TDA-PBE}}(\text{2T-7N}) = 0.199 \text{ eV}, \quad (14)$$

confirming these results the minor effect of the correlation potential, and kernel, for Kohn-Sham (KS) orbital shapes and energies [60, 61], although in the correct direction of decreasing the singlet-triplet gap. Note that for other dyes commonly employed in the TADF field (i.e., 2CzPN, ACRXTN, DABNA-1, and TABNA) these conclusions remain, with variations of less than 0.1 eV for ΔE_{ST} between TDA-PBEx and TDA-PBE, showing how this is indeed a general performance. The values for the $S_1 \leftarrow S_0$ and $T_1 \leftarrow S_0$ excitation energies at all the TDA-DFT level can be found as Sup-

plementary Material.

This is further corroborated by the HF-PBE calculation (i.e., within a TDA-DFT framework adding the PBE correlation functional to the full Hartree-Fock-like or exact-exchange term) from which we obtain rather similar values to CIS:

$$\Delta E_{ST}^{\mathrm{TDA-HF-PBE}}(\text{2T-N}) = 0.321 \text{ eV} \quad (15)$$

$$\Delta E_{ST}^{\mathrm{TDA-HF-PBE}}(\text{2T-4N}) = 0.648 \text{ eV} \quad (16)$$

$$\Delta E_{ST}^{\mathrm{TDA-HF-PBE}}(\text{2T-7N}) = 0.390 \text{ eV}. \quad (17)$$

Comparing now the results from Eqs. (6)-(8) and (12)-(14), we can observe the (negative) sign and magnitude (approximately half of the "exchange energy") of the $(ia|\hat{f}_{xc}|jb)$ term [62], although still leading to $\Delta E_{ST} > 0$ values. The use of a hybrid functional like PBE0 ($C_x = 1/4$) would just situate the ΔE_{ST} results between both extremes (i.e., CIS and TDA-PBE), as already found here and in previous publications too [20]: e.g. $\Delta E_{ST}^{\mathrm{TDA-PBE0}}(\text{2T-N}) = 0.219$ eV. The use of a higher weight (i.e., $C_x = 0.54$ for M06-2X [39]) does not bring any significant difference: $\Delta E_{ST}^{\mathrm{TDA-M06-2X}}(\text{2T-N}) = 0.195$ eV. Due to the disjoint nature of HOMO and LUMO, and since excited states are mostly HOMO to LUMO excitations in the single-excitation picture, these excitations could thus be viewed as intramolecular (short-range) charge-transfer excitations similarly as for DABNA-1 and TABNA compounds. Previous failures of TD-DFT for dealing with charge-transfer excitations were corrected using a long-range correction to the $E_{xc}[\rho]$ functional, with the ωB97XD model [40] one of the most successfully employed versions. However, to discard that the wrong prediction of the $\Delta E_{ST} < 0$ values is not a question of short- vs. long-range effects of the exchange-correlation potential, the application of this functional to e.g. 2T-7N in previous pub-

lications [21] also led to a positive $\Delta E_{ST}^{\mathrm{TDA-}\omega\mathrm{B97XD}}$(2T-7N) = 0.23 eV. In summary, it seems problematic to obtain a $\Delta E_{ST} < 0$ value with standard TD-DFT [63].

3.2 Single- and Multi-reference ab initio results

We first start analyzing the CIS(D) method, with double excitations partly included through the (D) correction [64], which should allow to quantify the importance of this correction if so. Actually, the trend is completely reversed with respect to CIS, see Table 1, significantly modifying $\Delta E_{ST}^{\mathrm{CIS}}$ by –0.62, –0.98, and –0.93 eV, for 2T-N, 2T-4N, and 2T-7N, leading respectively to new values of:

$$\Delta E_{ST}^{\mathrm{CIS(D)}}(\text{2T-N}) = -0.280 \text{ eV} \quad (18)$$

$$\Delta E_{ST}^{\mathrm{CIS(D)}}(\text{2T-4N}) = -0.288 \text{ eV} \quad (19)$$

$$\Delta E_{ST}^{\mathrm{CIS(D)}}(\text{2T-7N}) = -0.523 \text{ eV}. \quad (20)$$

The effect of double excitations for individual excited-state S_1 and T_1 energies is much more pronounced for S_1, with a rough decrease (stabilization) of –42 %, –35 %, and –38 %, for 2T-N, 2T-4N, and 2T-7N, respectively, compared with the corresponding values for T_1 of –7 %, –5 %, and –20 %, in agreement with previous studies [65]. However, the ΔE_{ST} values at the CIS(D) should be taken with some caution from recent benchmark studies in organic chromophores [66].

Therefore, we systematically assess the impact of high-order excitations by considering next some of the correlated methods applicable to excited-states such as SCS-CC2, SCS-ADC(2), SA-CASSCF, and SC-NEVPT2 to tackle these challenging systems. First of all, Table 1 also includes the re-

sults of the SCS-CC2 and SCS-ADC(2) methods, from which it can be consistently observe $\Delta E_{ST} < 0$ values for all the systems. Since CCS results, Coupled-Cluster with Single excitations, are similar to CIS, the (partial) introduction of double excitations by CC2 is again key to have those results. Note also that CIS(D) and SCS-corrected CC2 or ADC(2) methods rely on rather different theories and approximations, but individual $S_1 \leftarrow S_0$ and $T_1 \leftarrow S_0$ excitation energies are found in all cases in an excellent agreement between them, and with respect to the available experimental information. We also observe a close agreement between the CC2-based results and those values previously calculated at the EOM-CCSD level for 2T-N (1.09 and 1.19 eV, respectively [20]) and for 2T-7N (2.78 and 2.96 eV, respectively [21]). However, looking at the D_1 diagnostics [67] at the CC2 level, we found values around 0.08 for the three systems, and thus slightly higher than the threshold $D_1 \leq 0.05$ for which accurate results with respect to higher-order correlation methods are expected. Therefore, for the sake of completeness, we also apply next other family of methods.

Table 2 thus reports the results of systematically applying the SC-NEVPT2 method, with a pair of active spaces (minimal and large) to disentangle its effect (if any) on the results. The SA-CASSCF method (see the Supplementary Material) sometimes leads for these compounds to $\Delta E_{ST} > 0$ and sometimes to $\Delta E_{ST} < 0$ values, indicating that the introduction of non-dynamical correlation effects is not enough (although a first step) if one wants to deal with the intricate electronic effects of triangle-shaped systems due to its radicaloid nature [56]. The SC-NEVPT2 correction significantly decreases the SA-CASSCF results for $S_1 \leftarrow S_0$ and $T_1 \leftarrow S_0$ excitation energies of 2T-4N and 2T-7N, provinding in all cases very consistent results.

Looking at the radicaloid nature of the ground-state (S_0) of these systems, as given by the integrated number of electrons (N_U) housed on fractionally occupied orbitals [68–70], see details as Supplementary Material, we can see a transition from moderately (mono)radicaloid ($N_U = 0.75$ for 2T-N) to negligibly radicaloid ($N_U = 0.26$ character for 2T-7N), passing through an intermediate value of $N_U = 0.37$ character for 2T-4N.

Interestingly, when the dynamical correlation energy is introduced by the SC-NEVPT2 method, a value of $\Delta E_{ST} < 0$ for the singlet-triplet energy gap of all the systems is consistently obtained, in agreement with experimental and theoretical findings by the other methods explored before. Note also the quantitative agreement for individual $S_1 \leftarrow S_0$ and $T_1 \leftarrow S_0$ excitation energies between SC-NEVPT2 values and experimental estimates, a fact also corroborated before from benchmark calculations (pseudo-FCI results) of small systems [71]. This behaviour reflects the strong influence of "dynamic" correlation effects, introduced by the SC-NEVPT2 method, for achieving a $\Delta E_{ST} < 0$ value for 2T-7N. Furthermore, we also comment on the calculated $S_1 \leftarrow S_0$ oscillator strengths, for which negligible or very small values are observed [e.g. as much as $f = 4 \cdot 10^{-3}$ at the SC-NEVPT2(12,12) level for 2T-7N] in all cases and at all levels, leading essentially to dark states.

We investigate the weight of double- and higher-order excitations in the final CAS wavefunction of these systems. The CAS wavefunction is expressed as a linear combination of simply-, doubly-, triply-substituted, etc. Slater determinants, but with the excitation operator confined within the

subset of the selected active orbitals, as:

$$|\Psi_{\mathrm{CAS}}\rangle = \sum_{M} C_M|\Psi_M\rangle = C_0|\Psi_0\rangle + \sum_{i,a} C_i^a|\Psi_i^a\rangle + \sum_{ij,ab} C_{ij}^{ab}|\Psi_{ij}^{ab}\rangle + \sum_{ijk,abc} C_{ijk}^{abc}|\Psi_{ijk}^{abc}\rangle + \cdots , \tag{21}$$

with C_i^a, C_{ij}^{ab}, C_{ijk}^{abc}, etc. the corresponding coefficients of the expansion. The relative weight of the sum of C_{ij}^{ab}, C_{ijk}^{abc}, etc. coefficients reflects the importance of n-tuple excitations beyond single-particle ones. Note that for the S_0 wavefunction of all the systems, values of 6.2 %, 4.2 %, and 7.9 %, for 2T-N, 2T-4N, and 2T-7N, are calculated, respectively. Those weights are equal to 10.3 % (8.3 %) for the S_1 (T_1) excited-states of 2T-N, considerably higher than for other chromophores largely exploited as light-emitters for TADF applications [72]. For instance, for the compound 2CzPN, for which a $\Delta E_{ST} > 0$ value is theoretically and experimentally obtained, those weights roughly were 1.0 % and 0.7 %, respectively, at the SA-CASSCF level. For 2T-4N, and similarly to the case of 2T-N, we found values up to 10.1 % (8.4 %) for the S_1 (T_1) excited-states, and thus also slightly higher for the singlet than for the triplet wavefunction. Doubly-excited configurations are known to lead to a stabilization few times larger for singlet than for triplet excited-states, which supports the $\Delta E_{ST} < 0$ values obtained for 2T-N and 2T-4N essentially because Coulomb correlation primarily involves the interaction between anti-parallel spins [73, 74]. For 2T-7N, those values are 10.2 % (8.6 %) for the S_1 (T_1) excited-states, and therefore similar to 2T-N and 2T-4N.

3.3 Extension to other systems

We have also explored other systems as a *proof of concept* to confirm previous findings. First, the dicarboxylate derivative of 2T-N, see Figure 3,

namely 2T-N/COOH, for which experimental results are also available [54]. For this case, $S_1 \leftarrow S_0$ and $T_1 \leftarrow S_0$ experimental excitation energies are 1.07 and $<$ 1.16 eV, respectively, leading again to a very small (or possibly inverted) ΔE_{ST} value. Note that similar experimental results were found for monocarboxylate and nitrile derivatives of 2T-N, thus we will concentrate on the former molecule. Attaching the substituents did not significantly decrease the $N_U = 0.62$ value with respect to 2T-N, since the zig-zag edges housing reactive CH sites are not completely passivated [75]. We also obtain now $\Delta E_{ST} > 0$ values at the CIS and at all the TD-DFT levels, e.g. 0.22 eV (0.21 eV) at the TD-PBE0/def2-TZVP (TD-M06-2X/def2-TZVP) level, and $\Delta E_{ST} < 0$ values when CIS(D), SCS-CC2, or SCS-ADC(2) methods are instead employed (see Table 3). The SC-NEVPT2 method leads to very small ΔE_{ST} values oscillating about –0.02 and 0.02 eV. Actually, the relative weights of the double excitations for this system (5.6 %, 10.2 %, and 8.3 % from S_0, S_1, and T_1 CASSCF wavefunctions) are close to those obtained for the parent 2T-N compound, and thus also the results obtained.

A tricycloquinazoline compound related to 2T-4N, dubbed as 2T-4N/Ph_3 in Figure 3, is also studied to see the impact on extending the conjugated core [76]. In this occasion, all the methods predicted a $\Delta E_{ST} > 0$ value (see Tables 3 and 4) while obtaining relative weights of the double excitations for this system of the order of 14.1 % and 5.6 % from the S_1 and T_1 CASSCF wavefunctions, which are higher (S_1) or lower (T_1) than for the 2T-4N parent compounds. Perusing Table 3, one can see a considerable large ΔE_{ST} value at the CIS level, inferring thus a pronounced exchange energy hardly affected by any stabilization of the S_1 level driven by doubly-excited configurations, which is thus believed to be the reason for not having an inversion

of the S_1 and T_1 energy levels here. Note that for this compound a oscillator strength value of $f = 1.65 \cdot 10^{-2}$ was obtained at the SC-NEVPT2(12,12) level, compatible with a larger orbital overlap and thus with a $\Delta E_{ST} > 0$ value.

Next, the extension of the study to B-doped compounds, namely 2T-4B and 2T-7B, see Figure 3), would allow us to study the influence of the heterodoping. First of all, for 2T-4B a triplet ground-state (T_0) is predicted at some SC-NEVPT2 levels, which drops doubts about an excited-states energy inversion for this system. The substitution in heptazine of N by B atoms (at the same positions, see again Figure 3) serves to explore its B-doped analogue. The CIS calculation gave a ΔE_{ST} value of 0.23 eV, and thus even smaller than the one calculated for 2T-7N. Note that the S_1 and T_1 excited states are here of a $\pi \rightarrow n^{\star}$ nature, contrarily to a common $\pi \rightarrow \pi^{\star}$ transition in all the other molecules explored here, which decreases the orbital overlap and leads to a smaller value for ΔE_{ST}. The shape of the frontier occupied and virtual orbitals of 2T-7N and 2T-7B are compared in the Supplementary Material, with the LUMO, LUMO+1 and LUMO+2 of 2T-7B (all n-type) being very similar to HOMO-9, HOMO-8 and HOMO-7 of 2T-7N (all n-type). The same relative decrease going from 2T-7N to 2T-7B is observed applying TD-DFT, resulting in $\Delta E_{ST} > 0$ values such as 0.11 eV (0.08 eV) at the TD-PBE0/def2-TZVP (TD-M06-2X/def2-TZVP) levels. The application of CIS(D), SCS-CC2, or SCS-ADC(2) methods (see Table 3) also provided $\Delta E_{ST} > 0$ values of 0.08 and 0.10 eV, and thus very close to those obtained at the TD-DFT level in this case. The SC-NEVPT2 calculations provided negative (but very small) ΔE_{ST} values, see Table 4. For 2T-7B the contribution of the C_{ij}^{ab}, C_{ijk}^{abc}, etc. coefficients of the CASSCF

wavefunction is 0.8 %, 6.4 %, and 3.7 % for the S_0, S_1, and T_1 states, and thus lower than the values found for 2T-7N. Interestingly, comparing the SCS-CC2 and SC-NEVPT2 S_1 excited-state energies with respect to CIS values, taken as a baseline, we can see how S_1 is much more stabilized for 2T-7N than for 2T-7B, suggesting again a crucial role of dynamical correlation effects for achieving a more negative ΔE_{ST} value for 2T-7N than for 2T-7B, being able to overcome a larger exchange energy.

4 Conclusions

We have first studied the energy order of the lowest singlet S_1 and triplet T_1 excited-states of a set of N-doped (triangular shape) π-conjugated hydrocarbons, namely 2T-N, 2T-4N, and 2T-7N. The S_1-T_1 gap (referred as ΔE_{ST}) of these systems is expected to be negative, thus promoting exogernic reverse intersystem crossing processes, of interest within few fields where spin statistics still limit the efficiencies devices. Applying the TD(A)-DFT method, and independently of the exchange-correlation functional chosen, the S_1-T_1 gap is always found positive. We have, quantitatively and step by step, demonstrated that: (i) the correlation contribution is very small for both terms entering into the expression for ΔE_{ST}; and (ii) the term $(ia|\hat{f}_{xc}|jb)$ is negative compared to the positive $(ia|jb)$ value, which still leads to $\Delta E_{ST} > 0$ values. Values of $\Delta E_{ST} < 0$ are not expected to be reached due to the adiabatic approximation employed in common applications of TD(A)-DFT.

On the other hand, all the correlated *ab initio* methods explored, including CIS(D), SCS-CC2, SCS-ADC(2), SA-CASSCF, and SC-NEVPT2,

led to $\Delta E_{ST} < 0$ values for these systems, with the logical exception of CIS. The systematic investigation performed could isolate double (n-tuple) excitations, or more in general correlation effects, as key for correctly describing the S_1 and T_1 excited-states of 2T-N, 2T-4N, and 2T-7N. Nevertheless, this finding does not contradict the common strategy followed for D-A compounds, e.g. in OLEDs devices, relying on $S_1 \leftarrow S_0$ and $T_1 \leftarrow S_0$ intramolecular charge-transfer excitations, to achieve small ΔE_{ST} values. Actually, a pre-requisite for the S_1-T_1 inversion is to minimize the exchange energy, since then the greater stabilization of the S_1 than the T_1 excited-state by double excitations would allow to achieve the desired $\Delta E_{ST} < 0$ values.

Exploring other substituted (and realistic) 2T-N and 2T-4N molecules have allowed to confirm the previous conclusions for these N-doped systems. The case of 2T-7N (or heptazine is interesting, in the sense that the S_1 excited-state is also influenced by doubly-excited configurations in the CAS wavefunction. Interestingly, we note that the percentages associated with double and higher excitations is a necessary but not sufficient condition to observe a negative ΔE_{ST}. The effect of N vs. B substitution is also explored, and helped to corroborate the conclusions reached after studying the 2T-7B analogous molecule to 2T-7N, for which a smaller ΔE_{ST} value is found at the CIS level. However, the ΔE_{ST} values calculated by the rest of *ab initio* methods were not so affected by correlation effects, leading in that case to $\Delta E_{ST} \approx 0$ values.

In summary, we have shown both analytically and numerically, and by a variety of state-of-the-art methods for excited-states, the importance of elec-

tron correlation effects to predict the S_1-T_1 inversion in N-doped (triangular shape) π-conjugated hydrocarbons and some extension to other substituted compounds. These conclusion could stimulate further studies of compounds giving rise to negligibly small or even $\Delta E_{ST} < 0$ values, of relevance to photoactive materials, with carefully chosen electronic structure methods guiding their theoretical design.

Acknowledgements

The work in Alicante is supported by "Ministerio de Ciencia e Innovación" of Spain (Grant No. PID2019-106114GB-I00). Computational resources in Namur are provided by the "Consortium des Équipements de Calcul Intensif" (CÉCI), funded by the "Fonds de la Recherche Scientifiques de Belgique" (F.R.S.-F.N.R.S.) under Grant No. 2.5020.11. G.R. acknowledges a grant from the "Fonds pour la formation a la Recherche dans l'Industrie et dans l'Agriculture" (F.R.I.A.) of the F.R.S.-F.N.R.S.

Data Availability

The data that supports the findings of this study are available within the article [and its supplementary material] or are available from the corresponding author upon reasonable request.

Supplementary Material

The Supplementary Material contains in this order: (i) Individual $S_1 \leftarrow S_0$ and $T_1 \leftarrow S_0$ excitation energies, and the corresponding ΔE_{ST} value, at

10.1002/cphc.202000926

the TD-DFT level; (ii) Description of the FT-DFT method used to obtain the N_U values; (iii) Individual $S_1 \leftarrow S_0$ and $T_1 \leftarrow S_0$ excitation energies, and the corresponding ΔE_{ST} value, at the SA-CASSCF levels; (iv) Isocontour plots ($\sigma = 0.005$ e/bohr^3) of occupied and virtual orbitals of 2T-7B, calculated at the HF/def2-TZVP level, and comparison between molecular orbitals of 2T-7N and 2T-7B; and (v) Optimized cartesian coordinates of the compounds.

Table 1: Vertical excitation energies ($S_1 \leftarrow S_0$ and $T_1 \leftarrow S_0$, in eV) and associated singlet-triplet energy gap (ΔE_{ST}) calculated with different methods (and the def2-TZVP basis set) for the 2T-N, 2T-4N, and 2T-7N set of compounds.

Molecule	Method	$S_1 \leftarrow S_0$	$T_1 \leftarrow S_0$	ΔE_{ST}
2T-N	CIS	1.797	1.460	0.337
	CIS(D)	1.042	1.322	–0.280
	SCS-CC2	1.110	1.334	–0.224
	SCS-ADC(2)	1.080	1.308	–0.228
	Exp.[a]	0.97	0.93	0.04
2T-4N	CIS	3.211	2.526	0.685
	CIS(D)	2.106	2.394	–0.288
	SCS-CC2	2.258	2.342	–0.084
	SCS-ADC(2)	2.125	2.303	–0.178
	Exp.[b]	<2.39	2.29	<0.10
2T-7N	CIS	4.328	3.918	0.410
	CIS(D)	2.627	3.150	–0.523
	SCS-CC2	2.847	3.226	–0.379
	SCS-ADC(2)	2.790	3.174	–0.384
	Exp.[c]	–	–	<0

[a] Taken from Ref. 54.
[b] Taken from Ref. 55.
[c] Taken from Ref. 21.

Table 2: Vertical excitation energies ($S_1 \leftarrow S_0$ and $T_1 \leftarrow S_0$, in eV) and associated singlet-triplet energy gap (ΔE_{ST}) calculated with the SC-NEVPT2 method (and the def2-TZVP basis set) for the 2T-N, 2T-4N, and 2T-7N set of compounds.

Molecule	Method	$S_1 \leftarrow S_0$	$T_1 \leftarrow S_0$	ΔE_{ST}
2T-N	NEVPT2(6,6)	1.108	1.260	–0.152
	NEVPT2(12,12)	1.244	1.288	–0.044
	Exp.[a]	0.97	0.93	0.04
2T-4N	NEVPT2(6,6)	2.138	2.190	–0.052
	NEVPT2(12,12)	1.980	2.159	–0.179
	Exp.[b]	<2.39	2.29	<0.10
2T-7N	NEVPT2(6,6)	2.718	2.985	–0.267
	NEVPT2(12,12)	3.259	3.398	–0.139
	Exp.[c]	–	–	<0

[a] Taken from Ref. 54.
[b] Taken from Ref. 55.
[c] Taken from Ref. 21.

Table 3: Vertical excitation energies ($S_1 \leftarrow S_0$ and $T_1 \leftarrow S_0$, in eV) and associated singlet-triplet energy gap (ΔE_{ST}) calculated with different methods (and the def2-TZVP basis set) for the 2T-N/COOH, 2T-4N/Ph_3, and 2T-7B set of compounds.

Molecule	Method	$S_1 \leftarrow S_0$	$T_1 \leftarrow S_0$	ΔE_{ST}
2T-N/COOH	CIS	2.382	1.980	0.402
	CIS(D)	1.511	1.829	–0.318
	SCS-CC2	1.557	1.760	–0.203
	SCS-ADC(2)	1.538	1.743	–0.205
	Exp.[a]	–	–	< 0.1
2T-4N/Ph_3	CIS	4.338	2.782	1.556
	CIS(D)	3.707	3.503	0.224
	SCS-CC2	3.638	n.c.[b]	–
	SCS-ADC(2)	3.587	3.133	0.454
	Exp.[c]	–	–	≈ 0.4
2T-7B	CIS	2.629	2.396	0.233
	CIS(D)	2.125	2.044	0.081
	SCS-CC2	2.187	2.089	0.098
	SCS-ADC(2)	2.120	2.035	0.085

[a] Taken from Ref. 54.
[b] n.c. $\equiv$ not converged.
[c] Taken from Ref. 76.

Table 4: Vertical excitation energies ($S_1 \leftarrow S_0$ and $T_1 \leftarrow S_0$, in eV) and associated singlet-triplet energy gap (ΔE_{ST}) calculated with the SC-NEVPT2 method and the def2-TZVP basis set) for the 2T-N/COOH, 2T-4N/Ph_3, and 2T-7B set of compounds.

Molecule	Method	$S_1 \leftarrow S_0$	$T_1 \leftarrow S_0$	ΔE_{ST}
2T-N/COOH	NEVPT2(6,6)	1.566	1.688	–0.122
	NEVPT2(12,12)	1.793	1.817	–0.024
	Exp.[a]	–	–	< 0.1
2T-4N/Ph_3	NEVPT2(6,6)	3.608	3.192	0.416
	NEVPT2(12,12)	4.103	3.560	0.543
	Exp.[b]	–	–	≈ 0.4
2T-7B	NEVPT2(6,6)	3.724	4.013	–0.289
	NEVPT2(12,12)	2.094	2.149	–0.055

[a] Taken from Ref. 54.
[b] Taken from Ref. 76.

10.1002/cphc.202000926

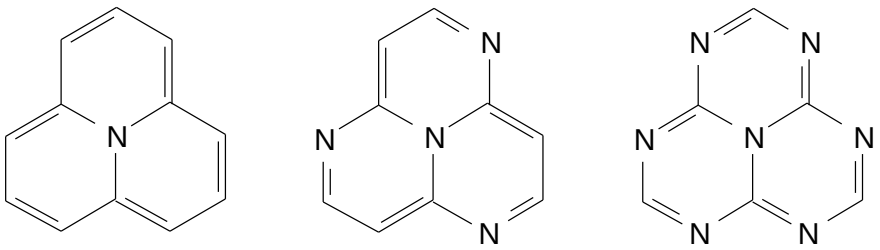

Figure 1: Chemical structure of studied molecules: 2T-N (or cyclazine), 2T-4N, and 2T-7N (or heptazine). Note that 2T refers to the number of hexagons per side, always forming a triangular shape molecule, and xN to the number of N atoms substituting C sites.

10.1002/cphc.202000926

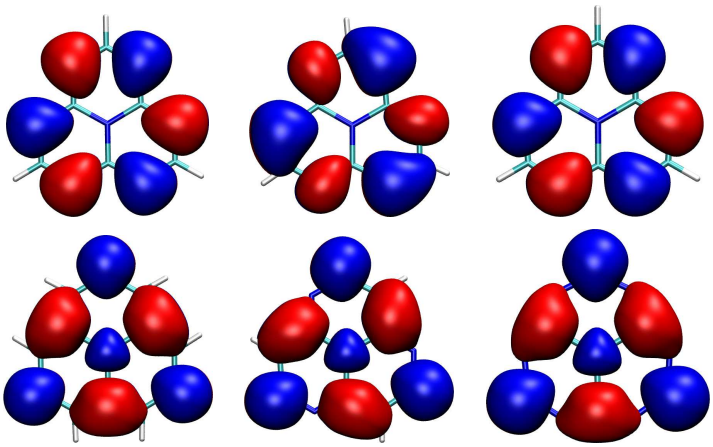

Figure 2: Isocontour plots ($\sigma = 0.005$ e/bohr^3) of HOMO (top) and LUMO (bottom) orbitals of 2T-N, 2T-4N, and 2T-7N, calculated at the HF/def2-TZVP level.

10.1002/cphc.202000926

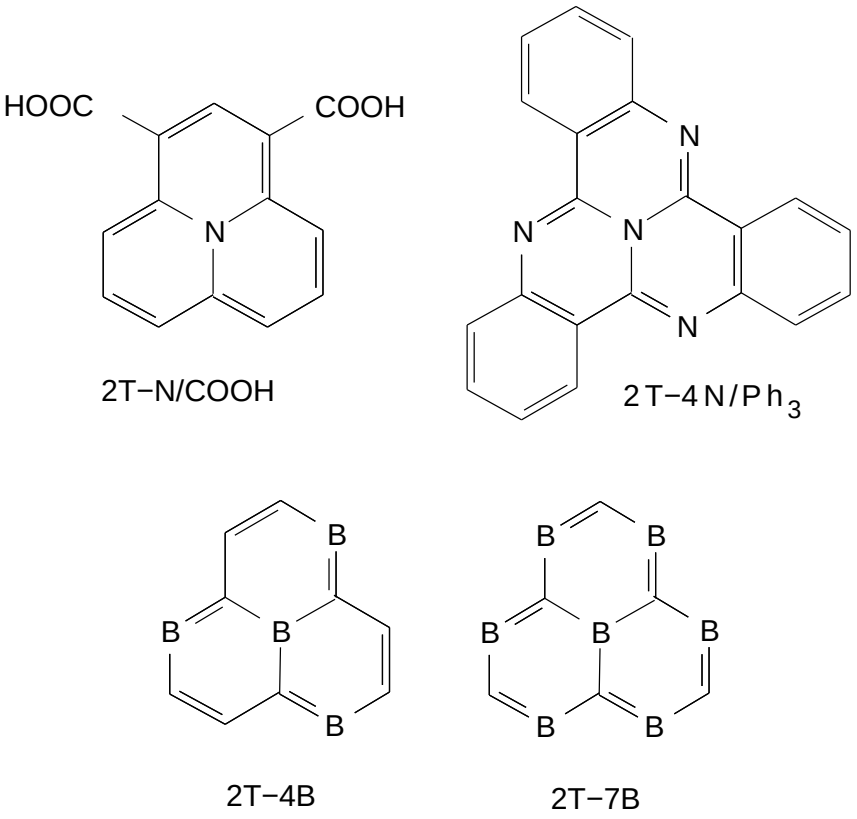

Figure 3: Chemical structure of studied molecules: 2T-N/COOH, 2T-4N/Ph_3, 2T-4B, and 2T-7B. Note that 2T refers to the number of hexagons per side, always forming a triangular shape molecule, and xN (xB) to the number of N (B) atoms substituting C sites.

References

[1] Ramachandra S Hosmane, Mitchell A Rossman, and Nelson J Leonard. Synthesis and structure of tri-s-triazine. *J. Am. Chem. Soc.*, 104(20):5497–5499, 1982.

[2] Dale R Miller, Dale C Swenson, and Edward G Gillan. Synthesis and structure of 2,5,8-triazido-s-heptazine: An energetic and luminescent precursor to nitrogen-rich carbon nitrides. *J. Am. Chem. Soc.*, 126(17):5372–5373, 2004.

[3] J Gracia and P Kroll. Corrugated layered heptazine-based carbon nitride: the lowest energy modifications of c_3n_4 ground state. *J. Mater. Chem.*, 19(19):3013–3019, 2009.

[4] Kamalakannan Kailasam, Johannes Schmidt, Hakan Bildirir, Guigang Zhang, Siegfried Blechert, Xinchen Wang, and Arne Thomas. Room temperature synthesis of heptazine-based microporous polymer networks as photocatalysts for hydrogen evolution. *Macromol. Rapid Commun.*, 34(12):1008–1013, 2013.

[5] Kamalakannan Kailasam, Maria B Mesch, Lennart Möhlmann, Moritz Baar, Siegfried Blechert, Michael Schwarze, Marc Schröder, Reinhard Schomäcker, Jürgen Senker, and Arne Thomas. Donor–acceptor-type heptazine-based polymer networks for photocatalytic hydrogen evolution. *Energy Technol.*, 4(6):744–750, 2016.

[6] Jie Li, Tetsuya Nakagawa, James MacDonald, Qisheng Zhang, Hiroko Nomura, Hiroshi Miyazaki, and Chihaya Adachi. Highly efficient organic light-emitting diode based on a hidden thermally activated de-

layed fluorescence channel in a heptazine derivative. *Adv. Mater.*, 25(24):3319–3323, 2013.

[7] Jie Li, Hiroko Nomura, Hiroshi Miyazaki, and Chihaya Adachi. Highly efficient exciplex organic light-emitting diodes incorporating a heptazine derivative as an electron acceptor. *Chem. Commun.*, 50(46):6174–6176, 2014.

[8] Takuji Hatakeyama, Kazushi Shiren, Kiichi Nakajima, Shintaro Nomura, Soichiro Nakatsuka, Keisuke Kinoshita, Jingping Ni, Yohei Ono, and Toshiaki Ikuta. Ultrapure blue thermally activated delayed fluorescence molecules: efficient homo–lumo separation by the multiple resonance effect. *Adv. Mater.*, 28(14):2777–2781, 2016.

[9] Soichiro Nakatsuka, Hajime Gotoh, Keisuke Kinoshita, Nobuhiro Yasuda, and Takuji Hatakeyama. Divergent synthesis of heteroatom-centered 4,8,12-triazatriangulenes. *Angew. Chem.-Int. Edit.*, 56(18):5087–5090, 2017.

[10] Kohei Matsui, Susumu Oda, Kazuki Yoshiura, Kiichi Nakajima, Nobuhiro Yasuda, and Takuji Hatakeyama. One-shot multiple borylation toward bn-doped nanographenes. *J. Am. Chem. Soc.*, 140(4):1195–1198, 2018.

[11] Mónica Moral, Luca Muccioli, W-J Son, Yoann Olivier, and Juan-Carlos Sancho-García. Theoretical rationalization of the singlet–triplet gap in oleds materials: impact of charge-transfer character. *J. Chem. Theory Comput.*, 11(1):168–177, 2015.

[12] Anton Pershin, David Hall, Vincent Lemaur, Juan-Carlos Sancho-García, Luca Muccioli, Eli Zysman-Colman, David Beljonne, and

Yoann Olivier. Highly emissive excitons with reduced exchange energy in thermally activated delayed fluorescent molecules. *Nat. Commun.*, 10(1):1–5, 2019.

[13] Adrien Zambon, J-M Mouesca, C Gheorghiu, Pierre-Alain Bayle, Jacques Pecaut, M Claeys-Bruno, Serge Gambarelli, and Lionel Dubois. s-heptazine oligomers: promising structural models for graphitic carbon nitride. *Chem. Sci.*, 7(2):945–950, 2016.

[14] Johannes Ehrmaier, Tolga NV Karsili, Andrzej L Sobolewski, and Wolfgang Domcke. Mechanism of photocatalytic water splitting with graphitic carbon nitride: photochemistry of the heptazine–water complex. *J. Phys. Chem. A*, 121(25):4754–4764, 2017.

[15] VR Battula, Sunil Kumar, DK Chauhan, Soumadri Samanta, and Kamalakannan Kailasam. A true oxygen-linked heptazine based polymer for efficient hydrogen evolution. *Appl. Catal. B-Environ.*, 244:313–319, 2019.

[16] Qin-Qin Dang, Yu-Fen Zhan, Xiao-Min Wang, and Xian-Ming Zhang. Heptazine-based porous framework for selective co_2 sorption and organocatalytic performances. *ACS Appl. Mater. Interface*, 7(51):28452–28458, 2015.

[17] Johannes Ehrmaier, Xiang Huang, Emily J Rabe, Kathryn L Corp, Cody W Schlenker, Andrzej L Sobolewski, and Wolfgang Domcke. Molecular design of heptazine-based photocatalysts: Effect of substituents on photocatalytic efficiency and photostability. *J. Phys. Chem. A*, 124(19):3698–3710, 2020.

[18] Anke Schwarzer, Tatyana Saplinova, and Edwin Kroke. Tri-s-triazines (s-heptazines)–from a "mystery molecule" to industrially relevant carbon nitride materials. *Coord. Chem. Rev.*, 257(13-14):2032–2062, 2013.

[19] Sunil Kumar, Neha Sharma, and Kamalakannan Kailasam. Emergence of s-heptazines: from trichloro-s-heptazine building blocks to functional materials. *J. Mater. Chem. A*, 6(44):21719–21728, 2018.

[20] Piotr de Silva. Inverted singlet–triplet gaps and their relevance to thermally activated delayed fluorescence. *J. Phys. Chem. Lett.*, 10(18):5674–5679, 2019.

[21] Johannes Ehrmaier, Emily J Rabe, Sarah R Pristash, Kathryn L Corp, Cody W Schlenker, Andrzej L Sobolewski, and Wolfgang Domcke. Singlet–triplet inversion in heptazine and in polymeric carbon nitrides. *J. Phys. Chem. A*, 123(38):8099–8108, 2019.

[22] Shmuel Zilberg and Yehuda Haas. Two-state model of antiaromaticity: The triplet state. is hund's rule violated? *J. Phys. Chem. A*, 102(52):10851–10859, 1998.

[23] Ganna Gryn'ova, Michelle L Coote, and Clemence Corminboeuf. Theory and practice of uncommon molecular electronic configurations. *Wiley Interdiscip. Rev.-Comput. Mol. Sci.*, 5(6):440–459, 2015.

[24] Ricardo Ortiz, Roberto A Boto, Noel García-Martínez, Juan C Sancho-García, Manuel Melle-Franco, and Joaquín Fernández-Rossier. Exchange rules for diradical π-conjugated hydrocarbons. *Nano Lett.*, 19(9):5991–5997, 2019.

[25] Piotr de Silva, Changhae Andrew Kim, Tianyu Zhu, and Troy Van Voorhis. Extracting design principles for efficient thermally acti-

vated delayed fluorescence (tadf) from a simple four-state model. *Chem. Mat.*, 31(17):6995–7006, 2019.

[26] MGUJ Petersilka, UJ Gossmann, and EKU Gross. Excitation energies from time-dependent density-functional theory. *Phys. Rev. Lett.*, 76(8):1212, 1996.

[27] Denis Jacquemin, Benedetta Mennucci, and Carlo Adamo. Excited-state calculations with td-dft: from benchmarks to simulations in complex environments. *Phys. Chem. Chem. Phys.*, 13(38):16987–16998, 2011.

[28] Adele D Laurent and Denis Jacquemin. Td-dft benchmarks: a review. *Int. J. Quantum Chem.*, 113(17):2019–2039, 2013.

[29] Carlo Adamo and Denis Jacquemin. The calculations of excited-state properties with time-dependent density functional theory. *Chem. Soc. Rev.*, 42(3):845–856, 2013.

[30] Jaspreet Kaur, Egor Ospadov, and Viktor N Staroverov. What is the accuracy limit of adiabatic linear-response tddft using exact exchange–correlation potentials and approximate kernels? *J. Chem. Theory Comput.*, 15(9):4956–4964, 2019.

[31] Patrick Kimber and Felix Plasser. Toward an understanding of electronic excitation energies beyond the molecular orbital picture. *Phys. Chem. Chem. Phys.*, 22(11):6058–6080, 2020.

[32] Mark E Casida. Time-dependent density-functional theory for molecules and molecular solids. *Theochem-J. Mol. Struct.*, 914(1-3):3–18, 2009.

[33] Barry Moore, Haitao Sun, Niranjan Govind, Karol Kowalski, and Jochen Autschbach. Charge-transfer versus charge-transfer-like excitations revisited. *J. Chem. Theory Comput.*, 11(7):3305–3320, 2015.

[34] So Hirata and Martin Head-Gordon. Time-dependent density functional theory within the tamm–dancoff approximation. *Chem. Phys. Lett.*, 314(3-4):291–299, 1999.

[35] Jan Gerit Brandenburg, Christoph Bannwarth, Andreas Hansen, and Stefan Grimme. B97-3c: A revised low-cost variant of the b97-d density functional method. *J. Chem. Phys.*, 148(6):064104, 2018.

[36] Rebecca Sure and Stefan Grimme. Corrected small basis set hartree-fock method for large systems. *J. Comput. Chem.*, 34(19):1672–1685, 2013.

[37] John P Perdew, Kieron Burke, and Matthias Ernzerhof. Generalized gradient approximation made simple. *Phys. Rev. Lett.*, 77(18):3865, 1996.

[38] Carlo Adamo and Vincenzo Barone. Toward reliable density functional methods without adjustable parameters: The pbe0 model. *J. Chem. Phys.*, 110(13):6158–6170, 1999.

[39] Yan Zhao and Donald G Truhlar. The m06 suite of density functionals for main group thermochemistry, thermochemical kinetics, noncovalent interactions, excited states, and transition elements: two new functionals and systematic testing of four m06-class functionals and 12 other functionals. *Theor. Chem. Acc.*, 120(1-3):215–241, 2008.

[40] Jeng-Da Chai and Martin Head-Gordon. Long-range corrected hybrid density functionals with damped atom–atom dispersion corrections. *Phys. Chem. Chem. Phys.*, 10(44):6615–6620, 2008.

[41] Celestino Angeli, Renzo Cimiraglia, S Evangelisti, T Leininger, and J-P Malrieu. Introduction of n-electron valence states for multireference perturbation theory. *J. Chem. Phys.*, 114(23):10252–10264, 2001.

[42] Celestino Angeli, Renzo Cimiraglia, and Jean-Paul Malrieu. N-electron valence state perturbation theory: a fast implementation of the strongly contracted variant. *Chem. Phys. Lett.*, 350(3-4):297–305, 2001.

[43] Celestino Angeli, Renzo Cimiraglia, and Jean-Paul Malrieu. N-electron valence state perturbation theory: A spinless formulation and an efficient implementation of the strongly contracted and of the partially contracted variants. *J. Chem. Phys.*, 117(20):9138–9153, 2002.

[44] Ove Christiansen, Henrik Koch, and Poul Jørgensen. The second-order approximate coupled cluster singles and doubles model cc2. *Chem. Phys. Lett.*, 243(5-6):409–418, 1995.

[45] Arnim Hellweg, Sarah A Grün, and Christof Hättig. Benchmarking the performance of spin-component scaled cc2 in ground and electronically excited states. *Phys. Chem. Chem. Phys.*, 10(28):4119–4127, 2008.

[46] Michael Wormit, Dirk R Rehn, Philipp HP Harbach, Jan Wenzel, Caroline M Krauter, Evgeny Epifanovsky, and Andreas Dreuw. Investigating excited electronic states using the algebraic diagrammatic construction (adc) approach of the polarisation propagator. *Mol. Phys.*, 112(5-6):774–784, 2014.

[47] Stefan Grimme. Improved second-order møller–plesset perturbation theory by separate scaling of parallel-and antiparallel-spin pair correlation energies. *J. Chem. Phys.*, 118(20):9095–9102, 2003.

[48] Frank Neese. Software update: the orca program system, version 4.0. *Wiley Interdiscip. Rev.-Comput. Mol. Sci.*, 8(1):e1327, 2018.

[49] TURBOMOLE V7.0 2015, a development of University of Karlsruhe and Forschungszentrum Karlsruhe GmbH, 1989-2007, TURBOMOLE GmbH, since 2007; available from `http://www.turbomole.com`.

[50] Florian Weigend and Reinhart Ahlrichs. Balanced basis sets of split valence, triple zeta valence and quadruple zeta valence quality for h to rn: Design and assessment of accuracy. *Phys. Chem. Chem. Phys.*, 7(18):3297–3305, 2005.

[51] Simone Kossmann and Frank Neese. Comparison of two efficient approximate hartee–fock approaches. *Chem. Phys. Lett.*, 481(4-6):240–243, 2009.

[52] Florian Weigend. Hartree–fock exchange fitting basis sets for h to rn. *J. Comput. Chem.*, 29(2):167–175, 2008.

[53] Laurent Galmiche, Clémence Allain, Tuan Le, Régis Guillot, and Pierre Audebert. Renewing accessible heptazine chemistry: 2,5,8-tris(3,5-diethyl-pyrazolyl)-heptazine, a new highly soluble heptazine derivative with exchangeable groups, and examples of newly derived heptazines and their physical chemistry. *Chem. Sci.*, 10(21):5513–5518, 2019.

[54] Werner Leupin and Jakob Wirz. Low-lying electronically excited states of cycl[3.3.3]azine, a bridged 12π-perimeter. *J. Am. Chem. Soc.*, 102(19):6068–6075, 1980.

[55] Werner Leupin, Douglas Magde, Gabriele Persy, and Jakob Wirz. 1,4,7-triazacycl[3.3.3]azine: basicity, photoelectron spectrum, photophysical properties. *J. Am. Chem. Soc.*, 108(1):17–22, 1986.

[56] María E Sandoval-Salinas, Abel Carreras, and David Casanova. Triangular graphene nanofragments: open-shell character and doping. *Phys. Chem. Chem. Phys.*, 21(18):9069–9076, 2019.

[57] Anna Köhler and David Beljonne. The singlet–triplet exchange energy in conjugated polymers. *Adv. Funct. Mater.*, 14(1):11–18, 2004.

[58] Begoña Milián-Medina and Johannes Gierschner. Computational design of low singlet–triplet gap all-organic molecules for oled application. *Org. Electron.*, 13(6):985–991, 2012.

[59] Yoann Olivier, Juan-Carlos Sancho-García, Luca Muccioli, Gabriele DAvino, and David Beljonne. Computational design of thermally activated delayed fluorescence materials: The challenges ahead. *J. Phys. Chem. Lett.*, 9(20):6149–6163, 2018.

[60] Ralf Stowasser and Roald Hoffmann. What do the kohn- sham orbitals and eigenvalues mean? *J. Am. Chem. Soc.*, 121(14):3414–3420, 1999.

[61] E San-Fabián and L Pastor-Abia. Dft calculations of correlation energies for excited electronic states using mcscf wave functions. *Int. J. Quantum Chem.*, 91(3):451–460, 2003.

[62] Kyungeon Lee and Dongwook Kim. Local-excitation versus charge-transfer characters in the triplet state: theoretical insight into the singlet–triplet energy differences of carbazolyl-phthalonitrile-based thermally activated delayed fluorescence materials. *J. Phys. Chem. C*, 120(49):28330–28336, 2016.

[63] Neepa T Maitra, Fan Zhang, Robert J Cave, and Kieron Burke. Double excitations within time-dependent density functional theory linear response. *J. Chem. Phys.*, 120(13):5932–5937, 2004.

[64] Andreas Dreuw and Martin Head-Gordon. Single-reference ab initio methods for the calculation of excited states of large molecules. *Chem. Rev.*, 105(11):4009–4037, 2005.

[65] Dongwook Kim. A theoretical understanding of the energy difference between singlet and triplet states of oligoacene molecules. *Int. J. Quantum Chem.*, 116(8):651–655, 2016.

[66] Charlotte Brückner and Bernd Engels. Benchmarking singlet and triplet excitation energies of molecular semiconductors for singlet fission: Tuning the amount of hf exchange and adjusting local correlation to obtain accurate functionals for singlet–triplet gaps. *Chem. Phys.*, 482:319–338, 2017.

[67] Curtis L Janssen and Ida MB Nielsen. New diagnostics for coupled-cluster and møller–plesset perturbation theory. *Chem. Phys. Lett.*, 290(4-6):423–430, 1998.

[68] Stefan Grimme and Andreas Hansen. A practicable real-space measure and visualization of static electron-correlation effects. *Angew. Chem.-Int. Edit.*, 54(42):12308–12313, 2015.

[69] Christoph Alexander Bauer, Andreas Hansen, and Stefan Grimme. The fractional occupation number weighted density as a versatile analysis tool for molecules with a complicated electronic structure. *Chem.-Eur. J.*, 23(25):6150–6164, 2017.

[70] Giovanna Salvitti, Fabrizia Negri, Ángel J Pérez-Jiménez, Emilio San-Fabián, David Casanova, and Juan Carlos Sancho-García. Investigating the (poly) radicaloid nature of real-world organic compounds with dft-based methods. *J. Phys. Chem. A*, 124(18):3590–3600, 2020.

[71] Pierre-François Loos, Martial Boggio-Pasqua, Anthony Scemama, Michel Caffarel, and Denis Jacquemin. Reference energies for double excitations. *J. Chem. Theory Comput.*, 15(3):1939–1956, 2019.

[72] Javier Sanz-Rodrigo, Yoann Olivier, and Juan-Carlos Sancho-García. Computational studies of molecular materials for unconventional energy conversion: The challenge of light emission by thermally activated delayed fluorescence. *Molecules*, 25(4):1006, 2020.

[73] H Kollmar and V Staemmler. Violation of hund's rule by spin polarization in molecules. *Theor. Chim. Acta*, 48(3):223–239, 1978.

[74] Shiro Koseki, Takeshi Nakajima, and Azumao Toyota. Violation of hund's multiplicity rule in the electronically excited states of conjugated hydrocarbons. *Can. J. Chem.*, 63(7):1572–1579, 1985.

[75] Andrés Pérez-Guardiola, María Eugenia Sandoval-Salinas, David Casanova, Emilio San-Fabián, AJ Pérez-Jiménez, and Juan-Carlos Sancho-Garcia. The role of topology in organic molecules: origin and comparison of the radical character in linear and cyclic oligoacenes and related oligomers. *Phys. Chem. Chem. Phys.*, 20(10):7112–7124, 2018.

[76] Robert B Cundall, David JW Grant, and Norman H Shulman. Photophysics of 5,10,14c,15-tetra-azabenzo[a]naphth[1,2,3-de]anthracene (tricycloquinazoline, tcq) and some of its derivatives. *J. Chem. Soc., Faraday Trans. 2: Mol. and Chem. Phys.*, 78(5):737–750, 1982.

10.1002/cphc.202000926

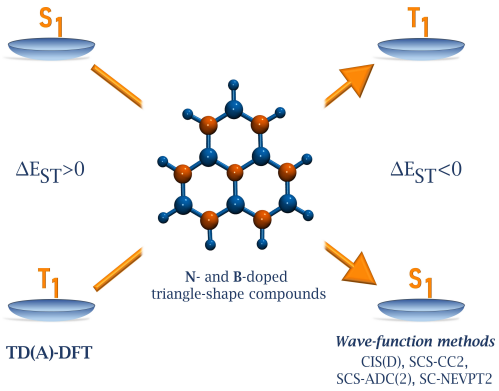

TOC figure: Inversion of S_1 and T_1 excited-states is made possible for N- and B-doped molecules, giving rise to an energy difference $\Delta E_{ST} < 0$ and thus to exogernic reverse intersystem crossing processes. This inversion is confirmed at CIS(D), SCS-CC2, SCS-ADC(2), and SC-NEVPT2 levels, while TD(A)-DFT was unable to predict it.